Efficient light-trapping nanostructures in thin silicon solar cells

Citation: Han, Sang Eon et al. "Efficient Light-trapping Nanostructures in Thin Silicon Solar Cells." Proc. SPIE 8031, Micro- and Nanotechnology Sensors, Systems, and Applications III, (May 13, 2011) Ed. Thomas George, M. Saif Islam, & Achyut K. Dutta. 2011. 80310T–80310T–9. CrossRef. Web.© (2011) COPYRIGHT Society of Photo-Optical Instrumentation Engineers (SPIE).

As Published: http://dx.doi.org/10.1117/12.881047

Publisher: Society of Photo-optical Instrumentation Engineers

Persistent URL: http://hdl.handle.net/1721.1/78296

Version: Final published version: final published article, as it appeared in a journal, conference proceedings, or other formally published context

Efficient light-trapping nanostructures in thin silicon solar cells

Sang Eon Han[1], Anastassios Mavrokefalos[1,2], Matthew Sanders Branham[1], and Gang Chen[1]*
[1]Department of Mechanical Engineering, Massachusetts Institute of Technology, 77 Massachusetts Avenue, Cambridge, MA 02139, USA
[2]Energy, Environment & Water Center, The Cyprus Institute, Nicosia, Cyprus

ABSTRACT

We examine light-trapping in thin crystalline silicon periodic nanostructures for solar cell applications. Using group theory, we show that light-trapping can be improved over a broad band when structural mirror symmetry is broken. This finding allows us to obtain surface nanostructures with an absorptance exceeding the Lambertian limit over a broad band at normal incidence. Further, we demonstrate that the absorptance of nanorod arrays with symmetry breaking not only exceeds the Lambertian limit over a range of spectrum but also closely follows the limit over the entire spectrum of interest for isotropic incident radiation. These effects correspond to a reduction in silicon mass by two orders of magnitude, pointing to the promising future of thin crystalline silicon solar cells.

Keywords: Light trapping, group theory, symmetry breaking, optical absorption, Lambertian limit

1. INTRODUCTION

Currently crystalline silicon (c-Si) yields the highest efficiency in single junction solar cells and constitutes ~80% of the solar cell market. However, for c-Si solar cells to replace fossil-fuel-based technologies, the cost of solar cells needs to be decreased by roughly a factor of three from the current ~$3.40 to ~$1.00 per Watt.[1] Even though cost will decrease as supply increases, current solar cell technologies should be advanced significantly in terms of device efficiency and manufacturing cost to achieve this cost goal. About a half of the total cost comes from the solar cell modules and the other half from installation.[1] Because both the module and installation cost can be decreased by the solar cell efficiency, increasing the efficiency is a key factor to reduce the total cost. The use of thin films can enhance the efficiency by reducing charge carrier recombination. Moreover, this strategy has the added advantage that the module cost can be decreased by using a less amount of materials. Typically, c-Si wafers 100-300 μm thick are used to ensure adequate absorption of sunlight and this material accounts for ~40% of the module cost.[2] While other more highly absorbing materials are used - such as amorphous silicon (a-Si), cadmium telluride (CdTe), or copper indium gallium diselenide (CIGS) - these materials suffer from their own limitations such as poor charge carrier collection, material scarcity, and material toxicity. Moreover, solar cells based on these materials have not achieved efficiencies as high as c-Si. Alternatively a significant reduction in cost can be realized, if c-Si with a thickness of a few microns can be made to absorb as efficiently as thick c-Si wafers. Therefore, the goal of this study is to design efficient light trapping structures in thin-film c-Si solar cells to enable the reduction of Si thickness in solar cells by around two orders of magnitude.

2. DESIGN OF PHOTONIC NANOSTRUCTURES

2.1 The Lambertian limit

Lambertian light trapping sets the thermodynamic limit of maximum absorption in a slab whose thickness is much larger than the wavelength of light.[3-5] This is attained when the surface is ideally rough such that the incident light is randomly scattered. In this case, compared to a flat surface, more light travels in the direction parallel to the wafer surface and optical path length increases. Thus light travels longer distances and optical absorption is enhanced as a result of a prolonged light-matter interaction time. With a lossless back reflector, the absorption enhancement factor becomes $4n^2$ compared to flat surfaces in the limit of weak absorption, where n is the refractive index of the film.[3] Conventionally, the $4n^2$ enhancement is known as the Lambertian limit or the Yablonovitch limit. In this case, absorptance A is obtained as[3]

*gchen2@mit.edu; phone 1-617-253-0006; fax 1-617-324-5519; web.mit.edu/nanoengineering

Micro- and Nanotechnology Sensors, Systems, and Applications III, edited by Thomas George, M. Saif Islam, Achyut K. Dutta, Proc. of SPIE Vol. 8031, 80310T
 · doi: 10.1117/12.881047

$$A = \frac{1}{1 + \frac{1}{4n^2 \alpha l}}, \tag{1}$$

where α is the absorption coefficient and l is the thickness of the film. Equation (1) assumes a perfect antireflection coating on the film and a perfect back reflector at all wavelengths. The absorptance in the Lambertian limit for a c-Si film of 2.012 μm thickness is shown in Fig. 1. If some optical elements are used that ideally allow light within an acceptance angle 2θ, the thermodynamic limit of light trapping is $4n^2/\sin^2\theta$.[5,6] This indicates that the Lambertian limit is the thermodynamic limit only for isotropically incident radiation which corresponds to $\theta=\pi/2$. For Si with a refractive index ~3.5, the $4n^2$ limit means that the path length can be increased by a factor of ~50. If this limit can be reached, the c-Si wafer thickness can be reduced from the current 100-300 μm to 1-3 μm, significantly reducing the material cost.

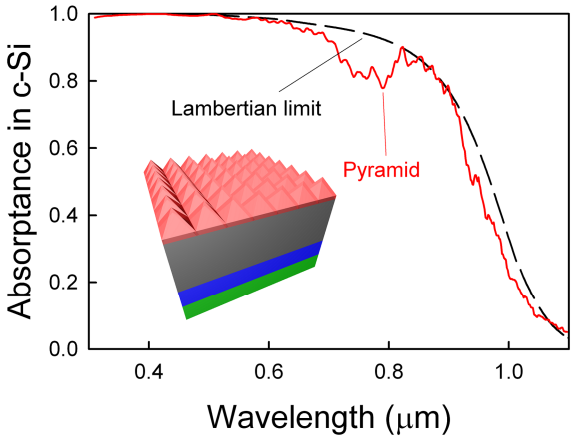

Figure 1. Absorptance of a pyramid structure. Red solid line represents absorptance of a pyramid structure. To smooth out the narrow peaks, the spectrum was averaged over $\Delta\lambda / \lambda^2 \sim 0.05$ μm^{-1}. Black dashed line represents the Lambertian limit of a c-Si film of equal thickness. The pyramid height and the length of its base are 566 and 800 nm, respectively. A 90-nm Si_3N_4 layer (red) is coated on the pyramids. The c-Si film (gray) thickness is 2.012 μm and a SiO_2 layer (blue) of thickness 717 nm is placed between the Si and the Ag back reflector (green).

Various schemes have been studied to enhance optical absorption in Si thin films including plasmonic scattering,[7] diffraction gratings,[8-11] and nanorod arrays.[12-15] However, previous work has not demonstrated how to approach the Lambertian limit when the film thickness is a few micrometers. Even at normal incidence, the absorption enhancement factor could exceed the Lambertian limit over very limited spectral ranges.[9-11] Typically, absorption decreases at other angles of incidence so that the angle-averaged spectrum is less than the Lambertian limit. The limit can be broken only when the photonic density of states (PDOS) exceeds that of the bulk. For example, PDOS can be increased by adding the contributions from evanescent waves and, in this way, the Lambertian limit can be broken for a film with a thickness of a few nanometers sandwiched between materials of higher refractive index.[16] However, high refractive index materials typically have a small band gap and absorb short wavelength light strongly, resulting in weak absorption in the sandwiched layer at short wavelengths. In this study, we consider how the Lambertian limit can be realized or even exceeded in structures that are a few micrometers thick to achieve absorptance comparable to thick c-Si wafers.

2.2 General design considerations

In order to design efficient light-trapping structures, we consider the optical properties of gratings. In general, the following three conditions will yield high performance gratings. First, two-dimensional gratings are preferred to one-dimensional ones, since two-dimensional gratings offer more diffraction channels.[9] Second, gratings couple well to incident light when they are tapered because the optical density varies gradually.[17] When used on the front surfaces, they can also decrease reflection.[18] Third, the grating period should be slightly smaller than the typical wavelength. If

the period is too small, light does not sense the structural details and optical diffraction is weak. When the period is larger than the wavelength, reflection orders higher than the zeroth order are possible, leading to a decrease in absorption. In this case, light is not confined well in the film but leaks through the higher-order channels.[16]

As an example, we consider pyramid structures with square bases. Prior studies of submicron pyramid structures considered relatively thick wafers.[19] Here we calculated absorptance for thickness ~2 μm using the transfer matrix method[20] and experimental values for the dielectric function.[21] The pyramid structures were optimized to obtain the maximum ultimate efficiency.[13,22] The ultimate efficiency η is defined as the maximum efficiency of a photovoltaic cell as the temperature approaches 0 K when each photon with energy greater than the band gap produces one electron-hole pair:

$$\eta = \frac{\int_0^{\lambda_g} I(\lambda)A(\lambda)\frac{\lambda}{\lambda_g}d\lambda}{\int_0^{\infty} I(\lambda)d\lambda}, \tag{2}$$

where I is the AM1.5G solar spectrum,[23] A the absorptance, λ the wavelength, and λ_g the wavelength corresponding to the band gap. Throughout this work, the absorptance calculations were performed for unpolarized light. Because of surface recombination issues, we fixed the ratio of the height to the base length of the pyramid to $1/\sqrt{2}$ which corresponds to the same surface area increase of $\sqrt{3}$ times over a flat film as in conventional c-Si solar cells. In all structures in this work, a SiO_2 film was placed between the Si layer and a Ag back reflector, and a Si_3N_4 antireflection layer of thickness 90 nm was coated on the Si structures. A number of absorptance peaks occurred in the spectra corresponding to waveguide resonances in the film.[5,9,10-13,16,17] The optimum period of the pyramid structure was found to be 800 nm which corresponds to the typical wavelength according to the third condition given above. The optimized absorptance spectrum at normal incidence is compared to the Lambertian limit in Fig. 1. Overall, the absorptance of the pyramid grating is not very far from the Lambertian limit. The performance of this structure is significant considering two points. First, an appreciable amount of light is absorbed in Ag at long wavelengths and only absorption in Si is accounted for in the calculations, while the Lambertian limit assumes a perfect metal. Second, the low reflectance of the pyramid structure at short wavelengths approaches the Lambertian limit which assumes perfect antireflection.

2.3 Symmetry-breaking

Although the pyramid structure is promising, we note that its absorptance is below the Lambertian limit over most of the spectrum even at normal incidence. To overcome this, we consider the symmetry properties of the pyramid structure. The point group symmetry of a unit cell of this structure contains a four-fold rotation axis and four mirror planes (see Fig. 2a). This symmetry remains the same when the cell is arranged in a square lattice as in our case. In general, symmetries result in degeneracy of the modes. More importantly, the presence of mirror planes results in certain modes not coupling to incident light.[24-26] To see this, let P_M be the operator that performs mirror reflection on a Bloch field in a structure with mirror symmetries. When it is operated on a Bloch vector field $\varphi_{\boldsymbol{k}}$ with a wave vector $\boldsymbol{k}$ that lies in the mirror plane, the resulting field satisfies the following equation:[27,28]

$$P_M\varphi_{\boldsymbol{k}} = \pm\varphi_{\boldsymbol{k}}. \tag{3}$$

Thus, the field can be either symmetric (+) or antisymmetric (–) under mirror reflection. Let the incident light be linearly polarized with an electric field $E_x\hat{\boldsymbol{x}}$, where $\hat{\boldsymbol{x}}$ is a unit vector in the x-direction. Mirror reflection operation on this field about the yz-plane results in $-E_x\hat{\boldsymbol{x}}$. Thus, the incident electric field is antisymmetric under the mirror reflection and the symmetric electric fields in the structure cannot be excited by the incident wave, leading to a decrease in absorption.

Group theory predicts[27] that, in our example, the modes can be classified into five categories according to their symmetries as shown in Fig. 2c where the magnetic fields in the z-direction are schematically drawn. The corresponding electric fields parallel to the xy-plane can be obtained by taking the curl of the magnetic fields according to the Maxwell's equation. Among the five, only one doubly degenerate mode (E) has the electric fields that are antisymmetric

under mirror reflection about the *xz*- or *yz*-plane and can couple to light. For another example, a hexagonal lattice where the unit cell contains a cylindrical or conical object has six mirror planes. The number of possible symmetries of modes in this case is six and the electric fields of only one of them (E_1) are antisymmetric under mirror reflection about the *xz*- or *yz*-plane as shown in Fig. 2d. Thus only this degenerate mode can couple to light. If all the six possible symmetries of modes occurred equally frequently over a range of spectrum, only a sixth of the modes would couple to light, resulting in a small number of absorptance peaks.

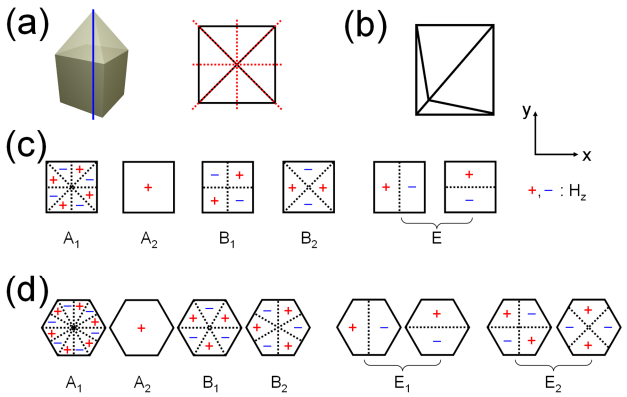

Figure 2. (a) Left: unit cell of the pyramid structure. The blue line is the four-fold rotation axis. Right: top view of the pyramid unit cell. Red dotted line represents mirror planes. (b) Top view of a skewed pyramid. (c),(d) H_z-field profile of the modes in a pyramid structure on a square lattice (c) and in structures with a six-fold rotation axis and six mirror planes (d), where the *z*-axis is normal to the paper. + and – represent the sign of the H_z-field and letters denote the irreducible representations of the electric field. The E representation (c), and the E_1 and E_2 representations (d) are doubly degenerate. Only the E (c) and E_1 (d) representations couple to light.

2.4 Skewed pyramid and skewed nanorod arrays

From the above observations, we note that the mirror symmetries need to be broken to improve absorption. One way to break symmetry is to destroy the periodic arrangement.[29] However, in this case the number of reflection channels increases at wavelengths where only zeroth order reflection is possible at perfect periodicity. This effect will decrease absorption. Thus, we distort the shape of the objects in the unit cell.[26,30] For example, we consider a skewed pyramid with a rectangular base as shown in Fig. 2b. When this nonsymmetric shape is arranged in a hexagonal lattice, no mirror planes exist. We optimized this structure to obtain the maximum efficiency. The ratio of the pyramid height to the longer side of its base was kept to $1/\sqrt{2}$ so that the surface area was approximately twice that of a flat surface. The optimized absorptance is shown in Fig. 3a. We observe that the absorptance of these skewed pyramids exceeds the Lambertian limit at normal incidence over a broad range of the spectrum. The calculated ultimate efficiency was slightly higher than the limit. Therefore, the effect of symmetry-breaking on absorption is significant. Note that this effect is related to optical phase. Because of the lack of structural symmetry, the optical phase of any mode cannot be symmetric or antisymmetric under mirror reflection and all modes couple to light in general. Thus this effect is different from absorption enhancement by symmetry-breaking of macroscopic structures[31] where optical phase information is absent.

Although the absorptance is high at normal incidence, we need to consider absorptance averaged over all incident angles to make a fair comparison to the Lambertian limit which is for isotropic incident radiation. Figure 3a shows that the angle-averaged absorption of the skewed pyramid grating is less than but close to the limit at long wavelengths and higher than non-skewed pyramids in Fig. 1 over most of the spectrum, especially long wavelength ranges. The enhancement over non-skewed pyarmids does not happen at short wavelengths where c-Si is strongly absorptive. In this region, many absorptance peaks broaden and overlap each other because of the short life times of the photonic modes. In this case, increasing the number of peaks by symmetry-breaking is not very effective in increasing absorptance over the spectral region. Rather, impedance matching between the incident light and the modes becomes more important to increase absorptance. The angular distribution of the ultimate efficiency is shown in Fig. 3b. In general, significant decrease in absorptance occurs at large polar angles (over 80 degrees) at which the sunlight does not usually shine the solar cell in practice.

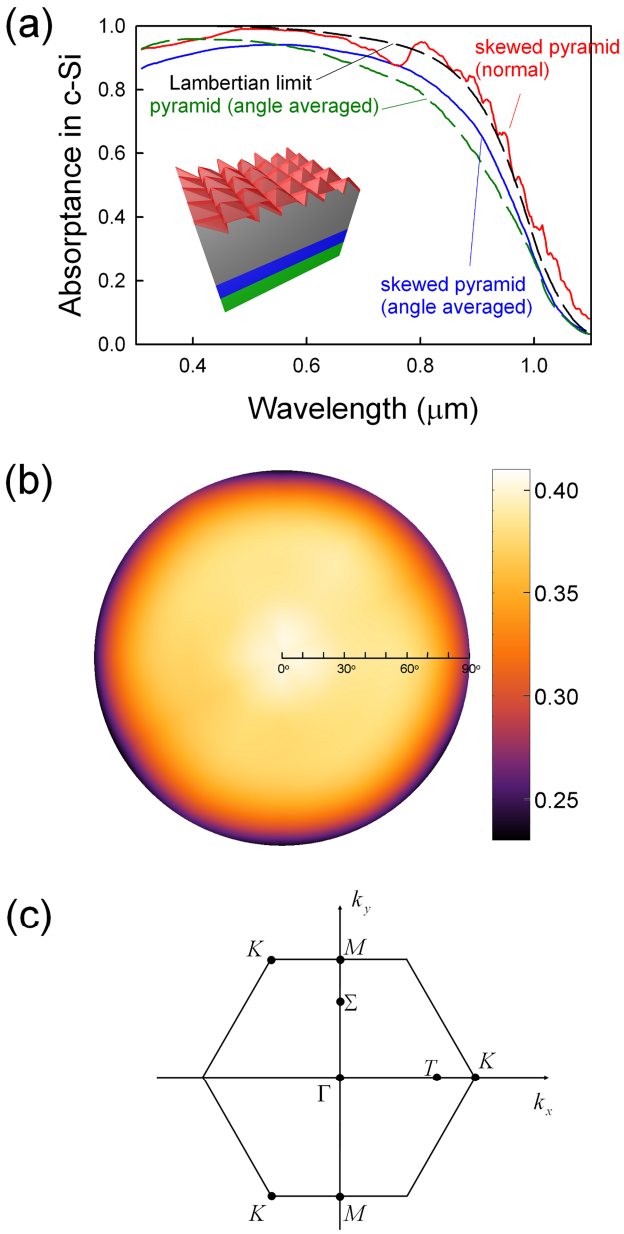

Figure 3. (a) Absorptance of a skewed pyramid structure at normal incidence (red solid line) and averaged over all directions of incidence (blue solid line). Angle-averaged absorptance of the pyramid structure in Fig. 1 is also shown (green dashed line). To smooth out the narrow peaks, the spectrum was averaged over $\Delta\lambda/\lambda^2 \sim 0.05\ \mu m^{-1}$. The black dashed line represents the Lambertian limit of a c-Si film of equal mass. The skewed pyramid height and the longer side of its base are 636 and 900 nm, respectively. A 90-nm Si_3N_4 layer (red) is coated on the skewed pyramids. The c-Si film (gray) thickness is 2.012 μm and a SiO_2 layer (blue) of thickness 741 nm is placed between the Si and the Ag back reflector (green). (b) Angular distribution of the ultimate efficiency of the skewed pyramids. The radial axis represents the polar angle. (c) The first Brillouin zone of a hexagonal lattice. The letters represent various symmetry points.

We note from Fig. 1 and 3a that the symmetry-breaking is not as effective at off-normal incidence as at normal incidence. This can be explained by considering symmetries when viewed at various directions. In Fig. 3c, the first Brillouin zone is drawn for a hexagonal lattice. According to group theory, the mirror reflection operations that leave a wave vector unchanged within reciprocal lattice vectors constitute the symmetry group for the field having the wave vector.[27] For example, the mirror plane at the *T* (Σ) point is the *xz*- (*yz*-) plane and the mirror planes at the *M* point are the *xz*- and *yz*-planes. At normal incidence of the Γ point, the symmetry group is the same as the lattice and six mirror planes exist. In general, symmetry is the highest at the Γ point and is lowered at other directions. Specifically, the number of mirror planes at the *T* (or Σ), *M*, and *K* point is one, two, and three, respectively, and an arbitrary point is nonsymmetric. Thus, breaking the structural symmetry is expected to be most effective at normal incidence, but is still advantageous near various high symmetry points. Because isotropic incident radiation includes these high symmetry points, symmetry-breaking can in general increase angle-averaged absorption.

We also investigated absorption as a function of the skewness of the pyramids at normal incidence. Figure 4 inset shows the top view of a unit cell which contains a pyramid. The red and blue dots denote the position of the pyramid vertex and the center of the unit cell, respectively. We define the pyramid skewness as the ratio between the distance of the vertex from the unit cell center (ξ) and a half of the diagonal of the unit cell (d). The pyramid skewness of 1 corresponds to the structure in Fig. 3a. We calculated the absorptance spectrum at different values of the pyramid skewness. The lattice constant, the pyramid height, and the Si_3N_4 coating thickness were kept constant. Figure 4 shows the ultimate efficiency as a function of the pyramid skewness. The ultimate efficiency changes monotonically from 37.4% to 39.9% as the pyramid skewness increases from 0 to 1 at normal incidence. From this figure, we can see not only the effect of symmetry-breaking on the ultimate efficiency but also the sensitivity of the efficiency to the changes in the structure.

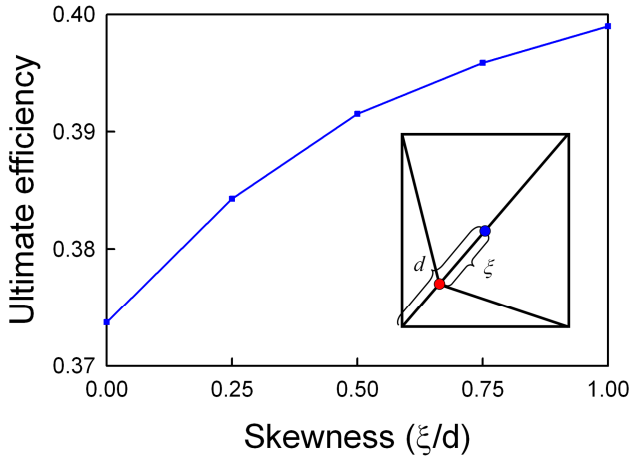

Figure 4. The ultimate efficiency as a function of the pyramid skewness defined in the text at normal incidence. The inset shows the top view of the pyramid. The lattice constant, the pyramid height, and the Si_3N_4 coating thickness are the same as in the structure in Fig. 3.

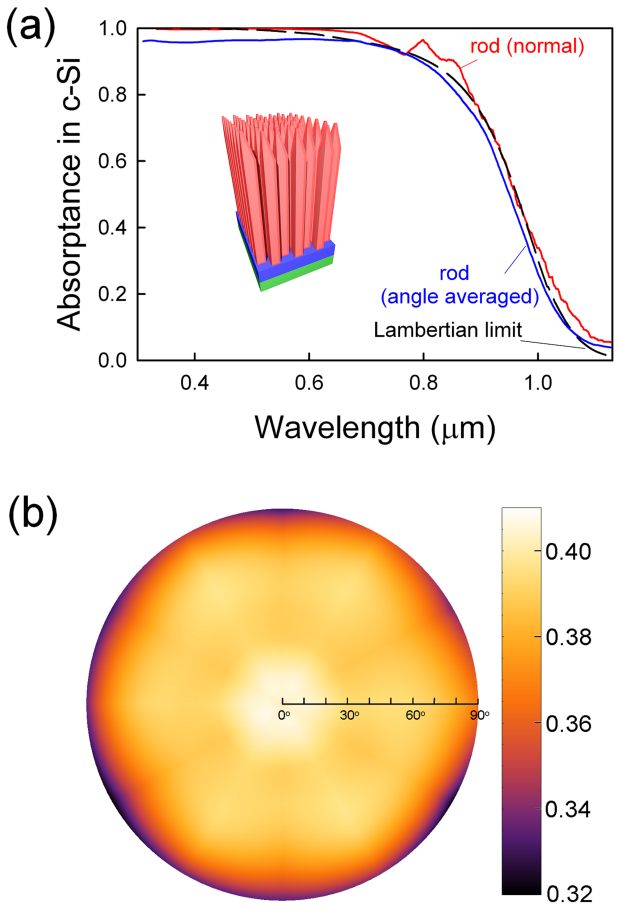

Figure 5. (a) Absorptance of the nanorod structure with skewed pyramids on its top at normal incidence (red solid line) and averaged over all directions of incidence (blue solid line). The pyramid height and the longer side of the base are 1125 and 450 nm, respectively. The length of the rod of rectangular cross section is 6.508 μm. A 90-nm Si_3N_4 layer (red) is coated on the tapered rods. A SiO_2 layer (blue) of thickness 953 nm is placed between the Si rod and the Ag back reflector (green). To smooth out the narrow peaks, the spectrum was averaged over $\Delta\lambda / \lambda^2 \sim 0.05\ \mu m^{-1}$. The black dashed line represents the Lambertian limit of a c-Si film of equal Si mass. The equivalent film thickness is 1.768 μm. (b) Angular distribution of the ultimate efficiency of the nanorods. The radial axis represents the polar angle.

To increase the angle-averaged absorption further, we consider a nonsymmetric nanorod array which has skewed pyramids at its top as shown in Fig 5a (inset). With this structure, the ultimate efficiency is above the Lambertian limit of a film of equal c-Si mass at normal incidence as seen in Fig. 5a. Moreover, the angle-averaged absorptance closely follows the Lambertian limit over the entire spectrum of interest. We also note that, at long wavelengths, the angle-averaged absorptance is even higher than the Lambertian limit over a limited spectral range, which is not possible for macroscopic rod structures where the density of photonic states is not modified by the structures.[5] For this rod structure, the angular distribution of the ultimate efficiency in Fig. 5b shows that the polar angle dependence is weaker than the skewed pyramids on a film. Because the angular distribution still bears some resemblance to six-fold rotation symmetry, the symmetry breaking might be pursued further.

To appreciate the absorption enhancement of the structures discussed above, we calculated their ultimate efficiencies as a function of the Si layer thickness in Fig. 6. Even though angle-averaged ultimate efficiencies are of interest, computations for all directions require a long time and we focus on normal incidence. In Fig. 6, we have added inverted pyramid structures which would be easy to fabricate. Figure 6 shows that to obtain the ultimate efficiency of a flat Si

wafer of thickness 100-300 μm, films of only 2-4 μm are needed for the skewed pyramids and the Si mass equivalent to 1-3 μm films are needed for nonsymmetric nanoroad structures (see the gray area). Moreover, the nonsymmetric rod array achieves efficiencies higher than the Lambertian limit at normal incidence over all thickness ranges of interest. Therefore, the simple technique of symmetry breaking makes it possible not only to realize the Lambertian limit in thin Si films but also to reduce the cost of c-Si solar cells significantly by decreasing the c-Si mass by two orders of magnitude. In general, the fabrication of the structures in Fig. 6 becomes more complicated as their light-trapping capability increases. This happens in the order of inverted pyramids, pyramids, skewed pyramids, and skewed nanorods. The light-trapping capability of the structures in Fig. 6 increases in the order of inverted pyramids, pyramids, skewed pyramids, and skewed nanorods. In general, the fabrication of the structures becomes more complicated in the same order, which implies a challenge that manufacturing cost might increase as more efficient structures are desired. Therefore, in order to minimize the overall cost of solar cells, it is important to develop scalable low-cost manufacturing processes for nonsymmetric nanostructures.

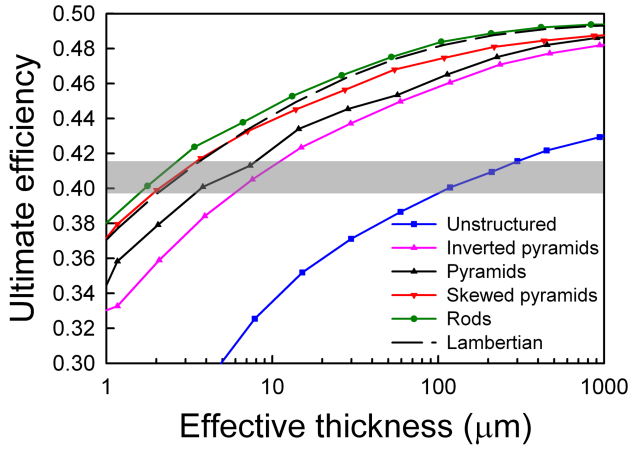

Figure 6. Ultimate efficiency of various structures as a function of their effective thickness for normal incidence. The effective thickness is the thickness of a film that has the same Si mass as the structures. For the rod structure, the actual length of the rods is ~4 times its effective thickness. The structural parameters of pyramids, skewed pyramids, and rods are the same as in Figs. 1, 3, and 5, respectively. The inverted pyramid height and the length of its base are 495 and 700 nm, respectively. A 90-nm Si_3N_4 layer is coated on the inverted pyramids and a Ag reflector is placed at the back of the c-Si film. The blue line represents an unstructured c-Si film with a Ag back reflector and a Si_3N_4 antireflection coating of thickness 61 nm. The gray area is the range of ultimate efficiency corresponding to an unstructured film of 100-300 μm.

3. CONCLUSION

We investigated light-trapping properties of periodic nanostructures in the wave optics regime. Using tapered two-dimensional gratings that are nonsymmetric, we showed that an absorptance close to the Lambertian limit at normal incidence is attainable. Further, we demonstrated that rod arrays with nonsymmetric tapered tops can exhibit absorptance that exceeds the Lambertian limit over a range of spectrum and is close to the Lambertian limit over the entire spectrum of interest even when averaged over all directions of incidence. This effect allows for the reduction of the crystalline silicon wafer thickness by two orders of magnitude, which suggests that thin crystalline silicon films can absorb light as efficiently as thick wafers.

ACKNOWLEDGMENT

This work was supported by NSF through UC Berkeley SINAM and through TeraGrid resources provided by Purdue University under Grant Number TG-PHY100046.

REFERENCES

[1] Lushetsky, J. The Prospect for $1/Watt Electricity from Solar, Department of Energy $1/W Workshop, 2010.
[2] Catchpole, K. R.; Polman, A. Opt. Express 2008, 16, 21793.
[3] Yablonovitch, J. Opt. Soc. Am. 1982, 72, 899.
[4] Stuart, H. R.; Hall, D. G. J. Opt. Soc. Am. A 1997, 14, 3001.
[5] Agrawal, M. Photonic Design for Efficient Solid-State Energy Conversion, Ch. 6, Ph.D. dissertation; Department of Electrical Engineering, Stanford University: Stanford, 2008.
[6] Campbell, P.; Green, M. A. IEEE Trans. Elect. Dev. 1986, ED-33, 234.
[7] Stuart, H. R.; Hall, D. G. Appl. Phys. Lett. 1996, 69, 2327.
[8] Sheng, P.; Bloch, A. N.; Stepleman, R. S. Appl. Phys. Lett. 1983, 43, 579.
[9] Bermel, P.; Luo, C.; Zeng, L.; Kimerling, L. C.; Joannopoulos, J. D. Opt. Express 2007, 15, 16986.
[10] Mallick, S. B.; Agrawal, M.; Peumans, P. Opt. Express 2010, 18, 5691.
[11] Zhou, D.; Biswas, R. J. Appl. Phys. 2008, 103, 093102.
[12] Hu, L.; Chen, G. Nano Lett. 2007, 7, 3249.
[13] Han, S. E.; Chen, G. Nano Lett. 2010, 10, 1012.
[14] Kelzenberg, M. D.; Boettcher, S. W.; Petykiewicz, J. A.; Turner-Evans, D. B.; Putnam, M. C.; Warren, E. L.; Spurgeon, J. M.; Briggs, R. M.; Lewis, N. S.; Atwater, H. A. Nature Mater. 2010, 9, 239.
[15] Garnett, E.; Yang, P. Nano Lett. 2010, 10, 1082.
[16] Yu, Z.; Raman, A.; Fan, S. Proc. Nat. Acad. Sci. U.S.A. 2010, 107, 17491.
[17] Chutinan, A.; Kherani, N. P.; Zukotynski, S. Opt. Express 2009, 17, 8871.
[18] Sai, H.; Fujii, H.; Arafune, K.; Ohshita, Y.; Kanamori, Y.; Yugami, H.; Yamaguchi, M.. Jpn. J. Appl. Phys. 2007, 46, 3333.
[19] Sai, H.; Kanamori, Y.; Arafune, K.; Ohshita, Y.; Yamaguchi, M. Prog. Photovoltaics 2007, 15, 415.
[20] Bell, P. M.; Pendry, J. B.; Martín-Moreno, L.; Ward, A. J. Comput. Phys. Commun. 1995, 85, 306.
[21] Handbook of Optical Constants of Solids; Palik, E. D., Ed.; Academic; Orlando, FL, 1985.
[22] Shockley, W.; Queisser, H. J. J. Appl. Phys. 1961, 32, 510.
[23] Air Mass 1.5 Spectra, American Society for Testing and Materials, http://rredc.nrel.gov/solar/spectra/am1.5/.
[24] Robertson, W. M.; Arjavalingam, G.; Meade, R. D.; Brommer, K. D.; Rappe, A. M.; Joannopoulos, J. D. Phys. Rev. Lett. 1992, 68, 2023.
[25] Ochiai, T.; Sakoda, K. Phys. Rev. B 2001, 63, 125107.
[26] Kilic, O.; Digonnet, M.; Kino, G.; Solgaard, O. Opt. Express 2008, 16, 13090.
[27] Inui, T.; Tanabe, Y.; Onodera, Y. Group Theory and Its Applications in Physics; Springer-Verlag: Berlin, 1990.
[28] Joannopoulos, J. D.; Johnson, S. G.; Winn, J. N.; Meade, R. D. Photonic Crystals: Molding the Flow of Light, 2nd ed.; Princeton University: Princeton, 2008.
[29] Chutinan, A.: John, S. Phys. Rev. A 2008, 78, 023825.
[30] Yu, Z.; Raman, A.; Fan, S. Opt. Express 2010, 18, A366.
[31] Campbell, P.; Wenham, S. R.; Green, M. A. Sol. Energy Mater. Sol. Cells. 1993, 31, 133.